

Segmentation through a local and adaptive weighting scheme, for contour-based blending of image and prior information.

D. Zarpalas^{†‡}, P. Gkontra[†], P. Daras[†], Member IEEE
[†] Informatics and Telematics Institute, Centre for
Research and Technology Hellas, Thessaloniki,
Greece. {zarpalas, gkontra, daras}@iti.gr

N. Maglaveras[‡], Senior Member IEEE
[‡] Medical Informatics Laboratory, Aristotle
University of Thessaloniki, Greece.
nicmag@med.auth.gr

Abstract

Active Contour Models have been widely used in computer vision for segmentation purposes, while anatomically constrained ACMs have offered a valuable solution on medical image segmentation, specifically for structures with weak boundaries. Efforts have been devoted on various ways of modeling prior knowledge, in terms of the morphology of the structures under investigation. This paper focuses on how to efficiently incorporate prior knowledge, into an ACM evolution framework, using the structures' distribution map as a second feature image, and blending the two images through a novel adaptive local weighting scheme. For proof of concept the method is applied on hippocampus segmentation in T1-MR brain images, a very challenging task, due to its multivariate surrounding region and the weak, even missing boundaries.

1 Introduction

Segmentation of anatomical structures in medical images is a topic of both major importance and challenge. Automatic segmentation of structures, could leverage systematic and extensive morphological analysis and shape comparisons of healthy and diseased subjects. Such analysis would indicate abnormal regions of a structure, thus lead to possible biomarker identification, disease prognosis and diagnosis, and optimum treatment identification. Research on the hippocampus-amygdala complex has shown that its morphology could indeed serve as a biomarker of mental diseases, e.g. Alzheimer's Disease (AD)[20, 9], even recognizing when Mild Cognitive Impairment could possibly lead to AD [22]. However, manual segmentation lacks reproducibility, while being time consuming and costly. On the other hand, automatic segmentation requires overcoming the inherent difficulties of medical imaging: noise and limited resolution, resulting to weak boundaries between

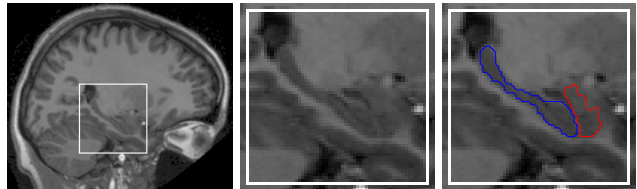


Figure 1. A sagittal slice of a brain MRI. The white box encloses the hippocampus and amygdala complex, while the blue and red contours depict the hippocampus and amygdala boundaries respectively.

neighboring structures of identical depiction values. Such a challenging example is the case of the hippocampus-amygdala complex, as Fig.1 shows.

ACMs have been widely used in the field of image segmentation; on an iterative evolution basis, specific energy amounts are evaluated until convergence. Evolution energies account either for the amount of gradient information on the contour, offering the edge-based ACMs, i.e. the Geodesic Active Contour proposed by Caselles [4], or for region homogeneity inside the contour contrary with the region outside the contour, offering the region-based ACMs, proposed by Chan and Vese [5]. Although a combination of both energies into a single hybrid framework is straightforward [23], the majority of recent medical imaging applications utilize the region-based technique, since it is more robust against noise, weak boundaries and smooth gradient edges. Due to these highly attractive properties, a lot of variations of the original region-based model have been proposed in the literature, e.g. in [16] a new variational level set formulation has been proposed that does not require re-initialization, while [26] proposed a formulation that has selective local to global behavior.

1.1 Incorporating Prior Knowledge

Pure ACMs solely depend on the image information and neglect any prior information. In the case of medical image segmentation though, prior information is critical, since even a human would not be able to distinguish the structures in an image, unless (s)he has been trained to recognize specific properties of the structures (e.g. shape). Thus, efforts have been devoted on ways to model such knowledge, since appropriate ways of modeling anatomical information for the purpose of segmentation could further be used for activation map extraction from fMRI analysis, as in [19]. Toward such modeling, statistical shape modeling was utilized to learn the shape characteristics of a given structure from a population. Cootes et al. [7] pioneered this field, known as Active Shape Models (ASMs), and proposed to learn a probability prior from a training set of shapes, by estimating a joint probability distribution over a set of landmarks on the shapes, using Principal Component Analysis (PCA). The learned shape prior was then used during the evolution of a deformable model, in order to constrain it over allowable shape variations, given the shapes of the population used in the training. The ASM concept of learning distribution of landmarks was extended to a more robust feature, the distance map. Distance maps constitute a form of implicit shape representation, as the level sets, and shape prior was firstly introduced to distance maps from Leventon et al. in [15]. Yang et al. [24], extended Leventon’s idea, and included within the shape prior a notion of neighborhood prior, for segmenting multiple neighboring structures, taking into account the shape inter-relationships among the neighboring structures. Furthermore, they managed to smoothly incorporate the prior information into the contour evolution process. The disadvantage of the above ASMs arises from the global character of PCA, that restricts dramatically the shape prior, especially when a small training set is employed, biasing the evolution towards the mean shape, as figure 2 shows. To overcome this disadvantage and have a less restrictive and local shape prior, Davatzikos et al. [10] proposed the use of wavelets on the contour and to divide it into spatiotemporal bands, on which PCA was applied. Nain et al. [17] applied this concept on the hippocampus, and extended it in 3D by using spherical wavelets.

Generalizing the ASM approach to include into the optimization framework the texture information, initially proposed by Cootes et al. in [8], has led to developing the Active Appearance Model (AAM), recently extended in [1] to include a graph-based matching, improving the initialization stage of the algorithm. In [14], AAMs based on level set evolution were proposed, in order to overcome the shortcomings of landmark based evolution. Readers are referred to [13] for a more thorough analysis on ways for statistical

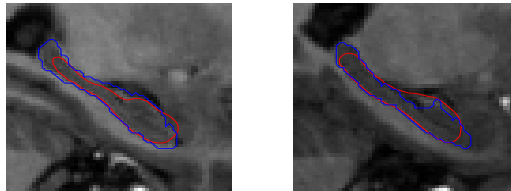


Figure 2. Two segmentation examples using PCA-based variational shape prior (red contour), contrary to actual boundary (blue). Long and thick hippocampus head is quite unlikely, hence PCA fails to capture it.

shape modeling of prior knowledge.

Another set of approaches on brain segmentation is based on atlas registration. In this framework, labels from the atlas, set manually, are propagated to the test image after a registration process between them is performed. Single atlas-based methods, have further been extended to multi-atlas, where each available labeled image is registered to the target, and the deformed labels from all of them are appropriately combined on the test image [12]. These methods are primarily differentiated by the registration’s nature; affine [6], piecewise affine [6, 2], or non-linear, e.g. [11], and the way of combining the multiple atlases.

1.2 Motivation

In this work, we present a different way of modeling prior knowledge, and more importantly a novel framework for embedding it into an ACM evolution process, by taking advantage of it in two different ways. Labeled images are used in a multi-atlas framework, to form the spatial distribution of hippocampus’ labels, i.e. an empirical probability map. This map is used in parallel with the target image and a region-based ACM is evolved on both, simultaneously. Thus, the energy minimization criterion encloses the image term (i.e. how well the contour fits the image) and the prior term (i.e. how likely the enclosed voxels belong to hippocampus). The second mean of prior knowledge’s exploitation is on how the two terms are blended during each evolution iteration. Previous solutions were merging the two terms in a global way, neglecting the fact that a given structure does have some more and some less trustworthy parts (i.e. parts where image information is sufficient or not), which are always at given anatomical locations. The hippocampus for example, has strong edge boundary on its bottom part, but weak on the head while it lacks any border with the tangent amygdala, due to the partial-volume effect at the resolution provided from a 1.5T MRI scanner. A human rater knows the parts where (s)he has to trust image information and where to trust his/her experience. Mimicking the humans segmentation concept, the authors have proposed a local weighting map for blending the

two terms, based on Gradient Distribution on the hippocampus' Boundary (GDB) [25], which offered very promising results. In this paper, this concept is further extended to become Adaptive (AGDB), based on the evolving contour, rather than based on a static local weighting map. This idea was motivated by the fact that a static map could not serve in full extend the variability of the hippocampus' shape, while on the other hand imitates even more the human understanding.

In the following Section our contributions on how to fully exploit prior knowledge are thoroughly explained. Experimental results in Section 3 verify the validity of the proposed concept, since better segmentation performance is achieved, compared to the existing variational shape prior technique and the previous implementation of the static GDB. Finally, conclusions are drawn in Section 4.

2 Proposed method

2.1 Spatial Distribution Map

In order to construct the statistical model of spatial class label distribution over the training set, the label images are used, where a label l has been assigned to each voxel \mathbf{v} , manually by an expert. Each labelled image L_n , $n = 1, \dots, N$ is a binary image, with $L_n(\mathbf{v}) = 1$ for voxels \mathbf{v} that belong to the hippocampus and 0 otherwise. Each of the N labeled images are non-rigidly registered on the test image. Registration is performed utilizing the algorithms of [21], and is based on the gradients of the test image and the training image, while the registration similarity score is then used as a weight. The weighted average of the registered L'_n , over the training population produces the Spatial Distribution Map L , which gives the empirical probability for every voxel of the specific test image $L(\mathbf{v}) = p(l_{\mathbf{v}}) \in [0, 1]$ to belong to hippocampus, based on its coordinates. Thus, SDM can assign to each voxel the probability to belong to the desired structure, based on its location. An ACM on L would try to separate the highly likely hippocampus' region from the unlikely one.

2.2 Energy terms

The utilized ACM framework is the region based from [5]: let Ω denote a bounded open subset of R^2 , with $\partial\Omega$ its boundary, and $C(s) : [0, 1] \rightarrow R^3$ is a parameterized curve in Ω . The curve C can be also implicitly represented via a Lipschitz function ϕ by $C = \{\mathbf{v} | \phi(\mathbf{v}) = 0\}$. C partitions Ω into the inside C set Ω_1 in which $\phi(\mathbf{v}) < 0$, and the outside C set Ω_2 in which $\phi(\mathbf{v}) > 0$. This region based framework is applied simultaneously on the test MR image I and on the SDM L , thus the same curve ϕ is evolved on the two images, capturing at the first one the region of voxels with consistent texture characteristics, while imposing

at the second one to be voxels with high spatial likelihood of belonging to hippocampus. For images I and L , both in the Ω domain, the Chan-Vese model is formulated by minimizing the following energy functionals:

$$\begin{aligned} E_I(M) &= \lambda_1 \int_{\Omega_1} M \circ |I(\mathbf{v}) - c_1^I|^2 d\mathbf{v} + \lambda_2 \int_{\Omega_2} M \circ |I(\mathbf{v}) - c_2^I|^2 d\mathbf{v} \\ E_L(M) &= \nu_1 \int_{\Omega_1} M \circ |L(\mathbf{v}) - c_1^L|^2 d\mathbf{v} + \nu_2 \int_{\Omega_2} M \circ |L(\mathbf{v}) - c_2^L|^2 d\mathbf{v} \end{aligned} \quad (1)$$

where $\mathbf{v} \in \Omega$, c_1^I, c_2^I and c_1^L, c_2^L are the average intensities of I and L in Ω_1 and Ω_2 respectively, while $\lambda_1, \lambda_2, \nu_1$ and ν_2 are balancing factors between the properties of interior and exterior regions. The operation \circ notates the Hadamard product, and the local weighting matrix M equals to the identity matrix in the analysis of [5].

2.3 Adaptive local weighting scheme

In order to model the human expert's segmentation methodology, of where and at which extend to trust either E_I or E_L , with respect to the hippocampus' body, we define the local weighting matrix, produced by adapting to the evolving contour the learned Gradient Distribution on the Boundary of the desired structure. Mean AGDB defines the density of the gradient values, on the mean shape of the hippocampus, thus which parts of the boundary demonstrate sufficient edge information, that one should trust. This distribution is adapted on every updated contour of the ACM framework, by registering ϕ_t to it. Hence, the name Adaptive Gradient Distribution on Boundary. This way, AGDB is aligned with the evolving contour, rather than with the SDM, as GDB does. Utilizing AGDB, the segmentation energy becomes:

$$E = E_I(AGDB) + E_L(1 - AGDB) \quad (2)$$

whose update equation reads:

$$\begin{aligned} \frac{\partial \phi}{\partial t} &= \delta_\epsilon(\phi) \left[\mu \operatorname{div} \left(\frac{\nabla \phi}{|\nabla \phi|} \right) - \nu \right. \\ &\quad \left. - AGDB_t \circ \left(\lambda_1 (I - c_1)^2 - \lambda_2 (I - c_2)^2 \right) \right. \\ &\quad \left. - (1 - AGDB_t) \circ \left(\nu_1 (L - d_1)^2 + \nu_2 (L - d_2)^2 \right) \right] \end{aligned} \quad (3)$$

where the first two regularization terms control the smoothness and the propagation speed, while the rest control the evolution forces.

The motivation of becoming adaptive, given the static GDB of [25] is illustrated in figures 3(a)-(c), where the local weighting map is imaged with white color on the regions where image information should be trusted¹. As Figure 3(c) shows, the static GDB cannot cover cases of hippocampuses

¹For the sake of demonstration, figures 3(d)-(f) depict (1-AGDB), i.e. dark values correspond to gradient-rich boundary parts, where image information should be trusted.

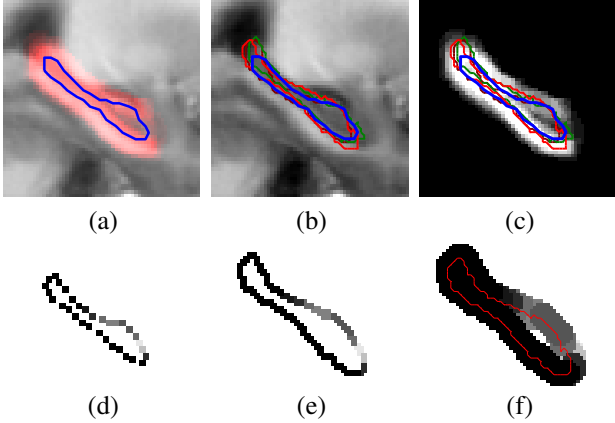


Figure 3. (a) GDB as a red overlay on the mean brain MR image and the mean hippocampus shape as blue contour. Three individual hippocampuses, plotted (b) over the mean MR image of the training dataset, and (c) over the static GDB map, with reference of the mean shape (blue). (d) Mean AGDB on 32 samples of the mean shape’s contour. Registered AGDB on the red contour of (c), before (e) and after (f) the dilation and smoothing.

with normal shapes, but having considerable deviation from the mean shape, as the upper left part in these cases falls on very low GDB values, which falsely translates that the algorithm should trust almost only prior information in those contours’ parts, since indeed there is strong image information.

2.4 Building AGDB

The adaptation procedure of the AGDB is illustrated in figures 3(d)-(f). In more detail, in order to construct the AGDB weighting map, the training set is used, and in every image the manually contour is outlined. Secondly, the canny edge detector [3] is applied and the binary intersection of the actual contour with the canny edge is extracted. Thirdly, the boundary is sampled on a prespecified amount of points along its contour. This process is repeated for every image of the set. Sampled contours are then registered to each other. Pairwise registration of contours C_1 and C_2 , is performed based on minimizing the differences of the contour samples’ distances from their centers.

$$\min_r \{ \hat{C}_1(s) - \hat{C}_2(s+r) \}, \text{ where } \hat{C} = C - \bar{C} \quad (4)$$

Registered sampled contours are then averaged, producing the mean AGDB depicted in figure 3(d), which is the offline outcome of the training procedure (along with SDM).

During active contour’s evolution, the mean AGDB is adapted on it, as figure 3(e) shows. Adaptation is achieved by registering the evolving contour and the mean AGDB, and upsampling. The final form for that evolution iteration

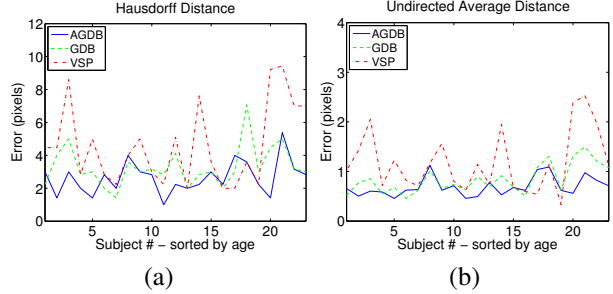


Figure 5. Comparisons based on (a) the Hausdorff distance, and (b) the undirected average distance.

$AGDB_t$, depicted in figure 3(f), is produced through successive dilations and smoothing.

3 Experimental Results

3.1 Evaluation Dataset

The proposed methodology has been tested on 23 T-1 weighted MP-RAGE MR images, randomly chosen from the OASIS database [18]. A professional radiologist manually traced the hippocampus volume on those 23 images, in order to build the training set. Apart from the OASIS pre-processing, the selected MR images were further rigidly registered on the hippocampus center of mass.

3.2 Comparisons

The proposed algorithm was evaluated in the context of the leave-one-out procedure. For every excluded test image, a new hippocampus spatial distribution map and AGDB map were generated. For comparison purposes, results of the previous GDB framework and of the combination of the Chan-Vese model with variational shape prior (abbreviated as VSP) have been calculated. The seeding region that initializes the evolutions was selected as the set of voxels with very high probability to belong to the hippocampus, i.e. high valued voxels of L .

The following results refer to segmentations performed on a central sagittal slice of each MRI. Performance and accuracy of the three comparing methods are evaluated through several metrics, i.e. the Hausdorff distance in figure 5(a), the undirected averaged distance in figure 5(b), precision vs recall in figure 6(a) and the F_1 measure in figure 6(b). Regarding the visualization of the Precision vs Recall diagram, the results of the proposed method are connected through colored segments with the ones produced by the static GDB and the VSP methods on the same MRI, showing AGDB’s tendency towards the optimum upper-right cor-

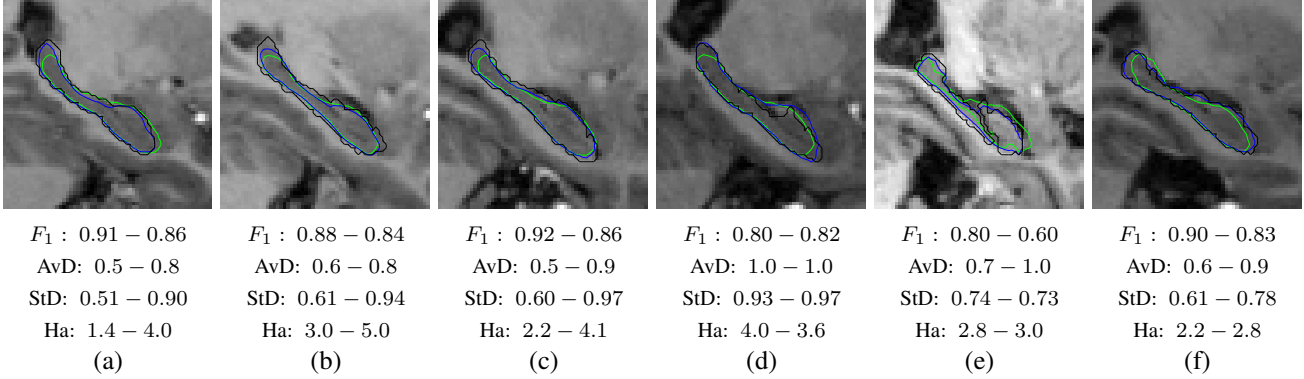


Figure 4. Segmentation results on images with age-sorted indexes 2, 3, 8, 12, 14 and 23, accompanied with the evaluation metrics (first value for AGDB and second for GDB). The thin black contour depicts the ground truth, while the blue one is the outcome of the proposed method and the green one of the static GDB method.

ner. F_1 equals the Dice coefficient, which measures set agreement: let H be the actual volume of the hippocampus, and \hat{H} the segmentation result, then F_1 equals:

$$F_1 = \frac{2|\hat{H} \cap H|}{|\hat{H}| + |H|} = \frac{2 \cdot Pr \cdot Re}{Pr + Re}, \quad F_1 \in [0, 1] \quad (5)$$

where Pr and Re refer to Precision and Recall, showing that F_1 actually offers a combined metric for both precision and recall. A value of $F_1 = 0$ indicates no overlap between the actual and estimated volume, while a value of $F_1 = 1$ indicates perfect agreement.

Table 1 shows averaged results for each of the evaluation metrics on the whole dataset, where the optimum value for each metric is written in bold; higher values for F_1 , Precision and Recall, while lower values for the undirected average distance error (AvD), its standard deviation (StD) and Hausdorff (Ha). The evaluation metrics verify the superiority of the proposed concept. While F_1 is widely used as a prime metric for segmentation performance, attention should be paid on the significant decrease of the distance errors, with very constrained standard deviation, showing that the proposed technique is more stable and robust.

Table 1. Averaged Comparison Results

	F_1	Pr	Re	AvD	StD	Ha
AGDB	0.86	0.85	0.88	0.70	0.70	2.65
GDB	0.82	0.82	0.84	0.84	0.82	3.29
VSP	0.79	0.83	0.78	1.18	1.20	4.59

Figure 4 shows examples of segmentation outputs on six cases, spanning on the complete aging axis. Figures 4 (a), (b), and (c) refer to the images whose contours are in figure 3(c). Note the difference in segmentation quality between the proposed method in (c) and (d) and the VSP method in figure 2 which are on the same MR images. These results verify the improvements on hippocampuses that have

large deviations from the mean shape, i.e. long and thick head and tail. The proposed method shows that is invariant on such cases. Example (d) is noteworthy, since the metrics for the two cases are quite close to each other, but do not seem to actually capture the very improved performance of AGDB contrary to static GDB, which has captured the long shape on both the head and the tail of the hippocampus. This is a nice example showing how the metrics assess the segmentation performance in a different way from the humans. A very challenging case is depicted in example (e), where the hippocampus is divided into two blobs. The AGDB result though fails to get separated, still shows better performance, neglecting many of the dark voxels that are in between them that GDB took into account. This figure by being very bright, contrary to the rest, further shows the invariance of the method on the different image intensity distributions.

4 Conclusions

The proposed method utilizes two terms in the evolution process; the regional intensity based on the Chan-Vese model and a prior knowledge term, a multi-atlas based empirical distribution of labels. The contribution of this paper is not only on how to model prior knowledge, but on how to combine it with the test image. A local weighting map, balancing on a voxel level the contribution of the two terms, has shown segmentation improvements. Adjusting it to the evolving contour throughout the segmentation process removes its static nature, utilizing the humans' adaptive understanding of which parts of the contour at hand represent the head or the tail of the hippocampus. Thus, AGDB imitates even more the way humans perform the segmentation procedure in general. The framework is not restricted nor fine-tuned on the hippocampus making it generic to other similar applications, where specific anatomical information is used during the segmentation.

Acknowledgements

The authors would like to thank the OASIS team [18] for providing their dataset and give special thanks to Angelos Baltatzidis M.D., Radiologist for building the training set, by manually outlining the hippocampus' contours.

References

- [1] K. Babalola, T. Cootes, "Using parts and geometry models to initialise Active Appearance Models for automated segmentation of 3D medical images", Biomedical Imaging: From Nano to Macro, 2010 IEEE International Symposium on , pp.1069-1072, 2010.
- [2] J. Barnes, R.G. Boyes, E.B. Lewis, J.M. Schott, C. Frost, R.I. Seahill, N.C. Fox, "Automatic calculation of hippocampal atrophy rates using a hippocampal template and the boundary shift integral", Neurobiology of Aging, Volume 28, Issue 11, Pages 1657-1663, 2007.
- [3] John Canny, "A Computational Approach to Edge Detection", IEEE Trans. on Pattern Analysis and Machine Intelligence, vol.8, no.6, pp.679-698, 1986.
- [4] V. Caselles, R. Kimmel, G. Sapiro, "Geodesic active contours", International Journal of Computer Vision, 22(1), 61-79, 1997.
- [5] T. Chan and L. Vese, "Active contours without edges", IEEE Trans. on Image Processing, vol. 10, pp. 2662-2677, 2001.
- [6] O.T. Carmichael, H.A. Aizenstein, S.W. Davis, J.T. Becker, P.M. Thompson, C. C. Meltzer, Y. Liu, "Atlas-based hippocampus segmentation in Alzheimer's disease and mild cognitive impairment", NeuroImage, vol. 27, Issue 4, Pages 979-990, 2005.
- [7] T.F. Cootes, C.J. Taylor, D.H. Cooper and J. Graham, "Active shape models-Their training and applications", Computer Vision and Image Understanding, vol 61, pp 38-59, 1995.
- [8] T. Cootes, G. Edward, C. Taylor, "Active appearance model", Proc. Eur. Conf. Computing and Visualization, 1998.
- [9] J.G. Csernansky, L. Wang, D. Jones, D. Rastori-Cruz, J.A. Posener, G. Heydenbrand, J.P. Miller, M.I. Miller, "Hippocampal Deformities in Schizophrenia characterized by high dimensional brain mapping", American Journal of Psychiatry, 159:12, 2002.
- [10] C. Davatzikos, X. Tao, and D. Shen, "Hierarchical active shape models, using the wavelet transform", IEEE Trans. on Medical Imaging, vol 22, no 3, 2003.
- [11] S. Gouttard, M. Styner, S. Joshi, R.G. Smith, H. C. Hazlett, and G. Gerig, "Subcortical structure segmentation using probabilistic atlas priors", SPIE Medical Imaging 2007: Image Processing, Volume 6512.
- [12] R.A. Heckemann, J.V. Hajnal, P. Aljabar, D. Rueckert, and A. Hammers, "Automatic anatomical brain MRI segmentation combining label propagation and decision fusion", NeuroImage, Volume 33, Issue 1, Pages 115-126, 2006.
- [13] Tobias Heimann and Hans-Peter Meinzer, "Statistical shape models for 3D medical image segmentation: A review", Medical Image Analysis, Volume 13, Issue 4, Pages 543-563, 2009.
- [14] S. Hu, D. L. Collins, "Joint level-set shape modeling and appearance modeling for brain structure segmentation", NeuroImage, Volume 36, Issue 3, 1 July 2007, Pages 672-683.
- [15] J. M. Leventon, E. Grimson, and O. Faugeras, "Statistical shape influence in geodesic active contours", in Proc. IEEE Conf. Comp. Vision Pattern Recognition, vol. 1, pp. 3163-323, 2000.
- [16] C. Li, C. Xu, C. Gui, and M. D. Fox, "Distance Regularized Level Set Evolution and its Application to Image Segmentation", IEEE Trans. Image Processing, vol. 19 (12), 2010.
- [17] Nain, D.; Haker, S.; Bobick, A.; Tannenbaum, A.; "Multiscale 3-D Shape Representation and Segmentation Using Spherical Wavelets", IEEE Transactions on Medical Imaging, vol.26, no.4, pp.598-618, April 2007.
- [18] D.S. Marcus, T.H. Wang, J. Parker, J.G. Csernansky, J.C. Morris, and R.L. Buckner, "Open Access Series of Imaging Studies (OASIS): Cross-Sectional MRI Data in Young, Middle Aged, Nondemented, and Demented Older Adults", Journal of Cognitive Neuroscience, 19, 1498-1507.
- [19] Wanmei Ou, William M. Wells III, and Polina Golland, "Combining spatial priors and anatomical information for fMRI detection", Medical Image Analysis, Volume 14, Issue 3, Pages 318-331, 2010.
- [20] M.E. Shenton, G. Gerig, R.W. McCarley, G. Szekely, and R. Kikinis, "Amygdala-hippocampal shape differences in schizophrenia: the application of 3D shape models to volumetric MR data", Psychiatry Research Neuroimaging, 115, 15-35, 2002.
- [21] H. Wang, L. Dong, J. O'Daniel, R. Mohan, A. S. Garden, K.K. Ang, D.A. Kuban, M. Bonnen, J.Y. Chang, and R. Cheung, "Validation of an accelerated 'demons' algorithm for deformable image registration in radiation therapy", Phys. Med. Biol. 50 (12), pp. 2887-2905, 2005.
- [22] R. Wolz, R.A. Heckeman, P. Aljabar, J.V. Hajnal, A. Hammers, J. Lötjönen, D. Rueckert and the Alzheimer's Disease Neuroimaging Initiative, "Measurement of hippocampal atrophy using 4D-graph cut segmentation: Application to ADNI", NeuroImage, 52, 109-118, 2010.
- [23] Y. Zhang, B.J. Matuszewski, L.K. Shark, C.J. Moore, "Medical image segmentation using new hybrid level set method", IEEE Int. Conf. on Biomedical Visualization, 2008.
- [24] J. Yang, L.H. Staib and J.S. Duncan, "Neighbor-Constrained Segmentation with Level Set Based 3D Deformable Models", IEEE Trans. on Medical Imaging, vol. 23(8), 2004.

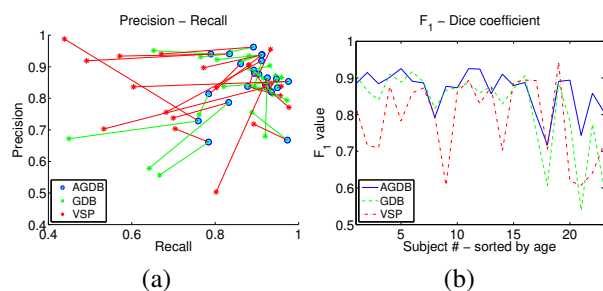


Figure 6. Comparisons based on Precision vs Recall plots and the F_1 /Dice coefficient. In (a), results on the same image of the GDB and VSP are connected with the ones from AGDB to reveal the tendency of the proposed method towards the optimum area of (1,1).

- [25] D. Zarpalas, A. Zafeiropoulos, P. Daras, and N. Maglaveras, "Hippocampus Segmentation using a Local Prior Model on its Boundary", International Conference on Machine Vision, Image Processing and Pattern Analysis, 2011.
- [26] K. Zhang, L. Zhang, H. Song, and W. Zhou, "Active contours with selective local or global segmentation: A new formulation and level set method", Image Vision Computing, 28(4): 668-676, 2010.